New quinoxaline 1,4-di-N-oxide derivatives:

Trypanosomaticidal activities and enzyme docking simulation

Yannick Estevez[1✣], Miguel Quiliano[2✣], Asuncion Burguete[3✣], Mirko Zimic[2], Edith Málaga[4], Manuela Verástegui[4] , Silvia Pérez-Silanes[3], Ignacio Aldana[3], Antonio Monge[3], Denis Castillo[2], Eric Deharo[1,5]

1. Université de Toulouse ; UPS ; UMR 152 (Laboratoire de pharmacochimie des substances naturelles et pharmacophores redox), 118, rte de Narbonne, F-31062 Toulouse cedex 9, France.

2. Bioinformatics Unit - Drug Design Group. Laboratorios de Investigación y Desarrollo. Facultad de Ciencias y Filosofía. Universidad Peruana Cayetano Heredia. Lima, Perú.

3. Unidad de Investigación y Desarrollo de Medicamentos, Centro de Investigación en Farmacobiología Aplicada (CIFA), University of Navarra, Campus Universitario, Pamplona, Spain.

4. Laboratorio de Enfermedades Infecciosas. Laboratorios de Investigación y Desarrollo, Facultad de Ciencias y Filosofía, Universidad Peruana Cayetano Heredia (UPCH), Av. Honorio Delgado 430, SMP, Lima, Peru.

5. IRD ; UMR-152 ; Mission IRD Casilla 18-1209 Lima, Peru.

✣*These authors* contributed equally *to this work and should be considered co-first authors.*

RECEIVED DATE (to be automatically inserted after your manuscript is accepted if required according to the journal that you are submitting your paper to)

CORRESPONDING AUTHOR FOOTNOTE

to whom correspondence should be addressed: phone (+ 51) 1-441-32-23. E-mail : eric.deharo@ird.fr

Abstract

Two series of pyrazol and propenone quinoxaline derivatives were tested for parasiticidal activity (against amastigotes of *Leishmania peruviana* and trypomastigotes of *Trypanosoma cruzi*) and for toxicity against proliferative and non-proliferative cells. The pyrazol series was almost inactive against *T. cruzi* but, 2,6-Dimethyl-3-[5-(3,4,5-trimethoxy-phenyl)-4,5-dihydro-1H-pyrazol-3-yl] - quinoxaline 1,4-dioxide inhibited 50% of *Leishmania* growth at 8.9 μM with no impact against proliferative kidney cells and low toxicity against Thp-1 and murine macrophages. The compounds of the propenone series were moderately active against *T. cruzi*. Among them, 2 compounds were particularly interesting: (2E)-1-(7-Fluoro-3-methyl-quinoxalin-2-yl)-3-(3,4,5-trimethoxy-phenyl)-propenone, that showed a selective activity against proliferative cells (cancer and parasites), being inactive against normal murine peritoneal macrophages and (2E)-3-(3,4,5-Trimethoxy-phenyl)-1-(3,6,7-trimethyl-quinoxalin-2-yl)-propenone that was only active against *Leishmania* and inactive against the other tested cells. Furthermore *in silico* studies were performed for ADME properties and docking studies, both series of compounds respected the Lipinski's rules and show linear correlation between tripanosomaticidal activities and Log*P*. Docking studies revealed that compounds of the second series could interact with the poly (ADP-ribose) polymerase protein of *Trypanosoma cruzi*.

Introduction

Leishmaniasis is a parasitosis occurring in visceral, cutaneous and mucocutaneous forms, affecting millions of people all around the world. Unfortunately, chemotherapy is limited to pentavalent antimonials, amphotericin B and pentamidine, that require injections, are toxic, expensive for most people in affected countries and have restricted therapeutic range in different clinical types of the disease[1]. Although miltefosine has been shown to be active by oral route in the treatment of Bolivian mucosal leishmaniasis[2], it is weakly active against other forms of leishmaniasis[3].

Chagas disease is also a public health problem but restricted to the South American continent. The acute phase of the disease causes severe myocarditis or meningitis while the chronic form may induce fatal heart failure[4]. Only few drugs are commercially available, but they are not consistently effective and all have serious side effects (including cardiac and/or renal toxicity).

As a result, the search for new trypanosomaticidal compounds remains essential to control and prevent the dramatically consequences of those parasitosis.

In a previous study[5] we showed that quinoxaline could pave the way to innovative antileishmanial drug candidates. We describe herein the Structure- Activity Relationship (SAR analysis) of trimethoxy-phenyl quinoxaline derivatives on amastigotes of *L. peruviana* (MHOM/PE/LCA08) infected peritoneal murine macrophages and on trypomastigotes of *Trypanosoma cruzi* (Tulahuen C4). Finally, we also studied *in silico* their ADME properties, putative mode of union and principal interactions with some essential trypanosomatidae protein targets.

Results and discussion

Biological activities

In this study, eleven quinoxaline derivatives were tested for their activity against various cell lines: three cancer cell lines (Vero, LLc-Mk2 kidney epithelial cell, and Thp-1 monocytic cells), one non-tumorogenic cell line (Murine Peritoneal Macrophages: MPM) and two parasites: amastigotes of *L. peruviana* (MHOM/PE/LCA08), responsible for cutaneous and sometimes mucocutaneous new world leishmaniasis and trypomastigotes of *Trypanosoma cruzi* (Tulahuen C4) responsible for Chagas disease,

a parasitosis only distributed through the American continent. The structure and biological activity of series 1 and 2 are presented in Table 1.

In a previous SAR study against *L. amazonensis*[5], with a series of ring substituted 3-phenyl-1-(1,4-di-*N*-oxide quinoxalin-2-yl)-2-propen-1-one derivatives (figure 1), we showed that the radical methoxy at position R_3', R_4' and R_5' was crucial to get leishmanicidal activity. Interestingly, the most active compound of the Burguete's series, i.e. (2E)-3-(3,4,5-trimethoxy-phenyl)-1-(3,6,7-trimethyl-1,4-dioxy-quinoxalin-2-yl)-propenone, was also the most lipophilic, had 3 methoxy radicals on the phenyl group and the R7 and R6 positions were occupied by methyl substituents. Cytotoxicity on macrophages revealed that this product was almost six times more active than toxic.

These observations led us to synthesize and test two closely related series: (1a-f) trimethoxy-phenyl pyrazol and (2a-f) trimethoxy-phenyl propenone quinoxaline derivatives.

As showed by Burguete et al.[5], the substitution in the R6 and R7 played a significant role in the lipophilicity and leishmanicidal activity of the studied compounds. In the first series (1a-f), when R6 and R7 positions were free (1a), cancer cells and MPM presented the same level of sensitivity, being 3 times less sensitive than amastigotes of *Leishmania* while trypomastigotes of *T. cruzi* were insensitive at doses up to 25 µM. On the contrary, when positions R6 and 7 were both occupied by a methyl (1f) the cytotoxicity increased on all the tested cells. Interestingly, whatever the substituent in R7 in the first series, MPM were almost insensitive. 1f was the only one of the series showing some (although moderate) activity against *T. cruzi* but it was also the most toxic on proliferative (and non) cell lines. 1b with a fluor in R7 (an electronegative atom), was two times more active than 1a against *L. peruviana* (Ic_{50}:13.7 µM). A methyl (1d and 1f) or a carbonyl (OCH3) (1e) led to non-toxic compounds against those cells. Interestingly, 1d (that was 2 times less lipophilic than 1f) was 2 times less effective on MPM and Thp-1 cells than 1f, and totally inactive against kidney cancer cell lines. 1d was the most active compounds of that series against *Leishmania* (Ic_{50}: 8.9 µM). Interestingly, this compound was inactive against Vero and LLc-Mk2 cells and almost 6 to 13 times more efficient on *Leishmania* than on Thp-1

or MPM. That is favourable in terms of selectivity. 1e was the lowest toxic (and also the lowest active against *L. peruviana*).

Globally, the first series of trimethoxy phenyl pyrazol quinoxaline (1a-f) derivatives showed a moderate activity against *L. peruviana* and was almost inactive against *T. cruzi* (except 1f slightly active).

The second series of trimethoxy phenyl propenone quinoxaline derivatives (2a-f) showed some moderate activity against *T. cruzi*. This series exhibited interesting activity against *L. peruviana*. 2a was the most toxic on all the tested cells and also the less lipophilic compound of the second series with the lowest selectivity index. On macrophages, a Cl (2c) or a F (2b) in R7 dropped the activity (almost 30 times less toxic than 2a). Compound 2b showed an interesting selective activity against proliferative cells (cancer and parasites) saving normal cells. It presented the best selectivity index, being 20 and 100 times more active against *T. cruzi* and *Leishmania* respectively than against MPM. In the case of *Leishmania* it was 2 times more selective than the control drug, Amphotericine B. A methyl (2d) also decreased the cytotoxicity but to a lesser extend (7 times less toxic than 2a): it showed a good activity against *L. peruviana* (Ic_{50}=5µM), and six-fold less toxic against MPM (Cc50 ~60µM). When the compound had a methyl in R6 and R7 (2f), i.e. a steric congestion on the benzenic cycle, the toxicity was restricted to *L. peruviana* (Ic_{50}=12.7 µM) and Thp-1 cells (Cc50 =38µM). On Thp-1 a Cl (2c) and a F (2b) decreased the toxicity. On that cells 2 methyl (2f) were much less cytotoxic (around 20 times). Vero and LLC-Mk2 cells reacted similarly, Cl (2c) did not affect the cells (while F in 2b, was almost 50 times more toxic). A R7-methoxy (2e) lead to a nine fold increased activity against *L. peruviana* with Ic_{50} values around 1µM and 10µM against *T. cruzi* but it was also the most cytotoxic ($Cc_{50} \leq 10\mu M$). The very good activity of 2e, could be due to the highest number of free rotable bonds allowing a better spatial layout (table 2). Compounds 2b and 2e were the most active against *L. peruviana* ($Ic_{50} \leq 3\mu M$) and *T.cruzi* ($Ic_{50} \leq 15\mu M$). However, compound 2e was twenty times more toxic on MPM, compared to 2b. That one, with a fluor in R7 exhibited a good activity against both *L. peruviana* (Ic_{50}~3µM) and *T. cruzi* (Ic_{50}~15µM) but it was quite toxic on the cancer lines (Thp-1, Vero and LLc-Mk2; Cc_{50}~20µM).

Interestingly it was not toxic against MPM (Cc_{50} >250μM). This specific activity against different cells in replication is probably due to a similar mode of action. Comparing *L. peruviana* and MPM, this compound, 2b, was almost 100 times more active against the parasite than against the MPM, turning it into the most interesting compound of the series. The compounds of the series 1 had a miLogP < 1, that means that these molecules are more hydrophilic than those of the series 2 with miLogP > 3.5. 1f was the most lipophilic and also the most toxic compound of the series 1, while 2f was the most lipophilic compound and the most selective of the series 2.

Correlations between LogP and the activities of the quinoxaline derivates

Simple Pearson correlation values, which are useful for measuring the association between two variables, were measured between Biological activities reported in table 1 and physical chemical property miLog*P* reported in table 2 for new quinoxaline derivates. As for the Burguete's series, among the newly synthesized compounds, an important element for the activity was also conferred by their lipophilicity, a crucial property for the crossing of cellular membranes. This is reflected in the correlation values reported for each activity and miLog*P*. Values reported clearly show a correlation between lipophilicity and Trypanosomaticidal activities expressed as Log ($1/Ic_{50}$) . Compounds in serie 1 followed a positive linear relationship (r = 0.94 in *L.peruviana* and not determinated in *T.cruzi*) while serie 2 a negative (r = -0.70 and r = -0.81) respectively.

Log*P* plays a fundamental role in the activity of the compounds and must be considering crucial such molecular descriptor in future sysntesis and QSAR studies. Predict computational analisis show the interactions between a protein and the compound 2b.

Computational analysis

General considerations

In a first *In silico* approach to discover a possible therapeutic target for this family of quinoxaline derivatives, the first priority was to find structural information related with complexes involving proteins and quinoxaline derivates, which means they share the same core quinoxaline and hence the same interactions characteristic of inhibitory capacity. In an exhaustive search, the Protein Data Bank

(PDB) screening showed three crystallized proteins complexing with quinoxaline-type compounds: The human poly (ADP-ribose) polymerase protein (PARP-1) (PDB ID: 1wok), the human c-Met Kinase (PDB ID: 3f66), and the human Kinase domain (PDB ID: 2zm4)[6, 7]. The above simple method has proved its usefulness providing numerous structural informations about potentially targets such human PARP-1 and conserved interactions reported in the bibliography for a typical PARP inhibitor. This and other information are detailed throughout the article.

A catalytic domain of PARP homologue in *T. cruzi* was found in the Sanger Institute Database (accession number Q4PQV7), and in the Genbank (accession number DQ061295). The *T. cruzi* catalytic domain of PARP is a 343 amino acids protein with 44% identity and 64.9% similarity with the human catPARP-1[8]. After blasting the *T. cruzi* databases against the two human kinases (PDB ID: 3f66 and 2zm4) meet in the protein search with quinoxaline inhibitor, no significant homologues were found. Only putative proteins with a partial low identity (29%) were detected. Alternatively, we only found two *T. cruzi* kinases, resolved by X-ray (1.9 Å and 2.1 Å resolution), of Arginine Kinase and glucokinase respectively (PDB ID: 2j1q and 2q2r)[9, 10].

Active site residues and typical interactions for PARP inhibitors.

The quality of the modeled T. cruzi catPARP-1 (figure 2a) passed through the multiple tests from the What-if and Prochek servers. The RMSD (root mean square deviation) between the T. cruzi catPARP-1 homologue model and the human catPARP-1 used as template was 0.07 Å.

It has been suggested that human catPARP-1 has a two-domains active site: a proton acceptor and a proton donor site11. Several inhibitors have been shown to bind to the donor site of the human catPARP-1, sharing a conservative pattern of interactions12. These interactions include hydrogen bonds with Gly863 (Gly446 in the T. cruzi catPARP-1) and stacking hydrophobic interaction consisting of a (π-π) interaction with Tyr907 and Tyr869 (Tyr490 and Tyr472 in T. cruzi). These amino-acids are highly conserved, in both sequence and structure 13 (figure 2b).

Analysis of potential candidate targets for 2a-f Quinoxalines

In previous studies[12], especially those on QSAR for PARP-1, it has been shown that molecular descriptors that better described the compound's activity were the Van der Vaals forces and the number of rotatable links. Van der Vaals reflects that the larger the surface of contact between ligand and active site the more potent could be the inhibition; while the number of rotable links was the opposite in view of the unfavourable entropy change after the ligand-active site interaction. The negative docking energy scores indicated more stable interaction between compounds 2a-2f and enzymes catPARP-1, Arginine Kinase and Glucokinase of *T.cruzi* (Table 3).

In the majority of cases, the conformations calculated for compounds are in agreement with the interactions[9] reported in different studies[8, 12, 13]. Nevertheless, the compounds 2d and 2e did not reproduce the typical interactions of an inhibitor of catPARP-1; related compounds 2f and 2e did not report the typical interactions with their substratum. The affinity values observed for the tested compounds (Gibbs free energy change, Table 3) to the respective proteins, showed more affinity for catPARP-1, followed by the Arginine Kinase and finally Glucokinase.

Conclusion

Against trypomastigotes forms of *T. cruzi*, the series 1 was almost inactive while the second series presents a moderate activity. The low activity of the tested compounds against *T. cruzi* compared with *Leishmania* could be explained because trypomastigotes are not reproductive forms instead of amastigote that are proliferative forms.

Against *Leishmania* parasite, 1d and 2f showed interesting selective activity with no impact against proliferative kidney cells and low toxicity against Thp-1 and MPM. For the second series (2 a-f), the hydrophilicity-lipophilicity balance seems to play an important role. The more hydrophilic the substituants were, the higher the antiparasitic activity and toxicity were (2e and 2b); the more lipophilic the substituants were, the more specific the antiparasitic effect was (2c and 2f). The electronegativity of substituants in R7 and R6 position played also a crucial role on selectivity, the most electronegative radicals (F, 2b and O-CH3, 2e) being the strongest but also the least selective activities. Both series of compounds respected the Lipinski's rules as they all have a molecular weight under 500 Daltons,

a limited lipophilicity (expressed by Log P < 5, with P = [drug] org./[drug]aq.), far less than 5 H-bond donors (expressed as the sum of OHs and NHs), and also far less than 10 H-bond acceptors (expressed as the sum of Os and Ns). Both series presented also a high percentage of absorption (%ABS), all compounds being then potentially able to cross biological membranes.

Although screening of proteins co-crystallized with quinoxaline family compounds threw 10 possible proteins, only 3 were taken into account, because they are of much interest for our laboratory. In the modeled protein, we observed that the cavity corresponding to the active site is larger than the one found in the human catPARP-1 (PARP-1 human : 790.67 $Å^2$, 1306.67 $Å^3$; PARP-1 T.cruzi: 965.09 $Å^2$, 1560.37 $Å^3$, calculated using CASTp server[14]) that could explain the selectivity of the *T. cruzi* catPARP-1.

The correlation between the Gibbs free energy and Ic_{50} was negative (r = -0.79), although the homology model was done at low resolution (3Å), the calculated Gibbs free energies suggest that catPARP-1 *T. cruzi* could be a potential target for the studied quinoxalines derivatives.

Finally, because of their property and selectivity, three molecules (1d, 2b and 2f) should be considered as good candidates for oral administration and should be evaluated *in vivo* against *Leishmania* infected mice. These results corroborate the results described by Burguete et al.[5] in *L. amazonensis* infected macrophages, as the most active compounds were a (R6-R7) dimethyl and a fluor (R7) substituted propenone quinoxaline.

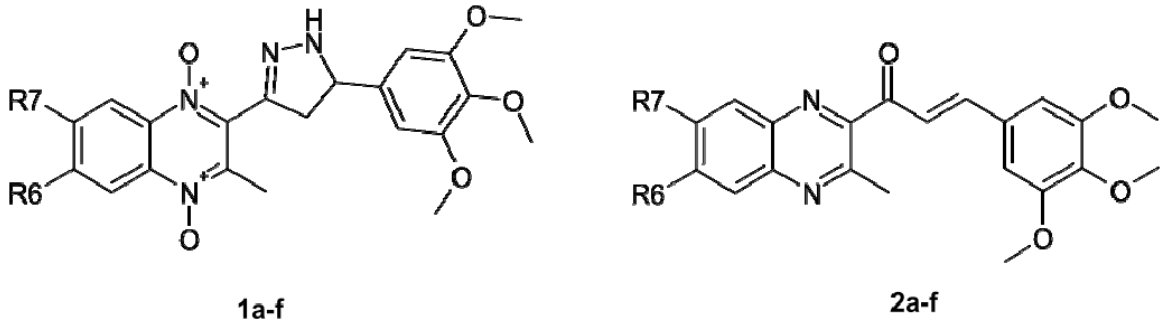

1a-f **2a-f**

R6/R7= H/H (**a**); H/F (**b**); H/Cl (**c**); H/CH_3 (**d**); H/OCH_3 (**e**); CH_3/CH_3 (**f**)

Figure 1.

Left: 3-phenyl-1-(1,4-di-N-oxide quinoxalin-2-yl)-2-propen-1-one derivatives described in Burguete and al. 2008[5].

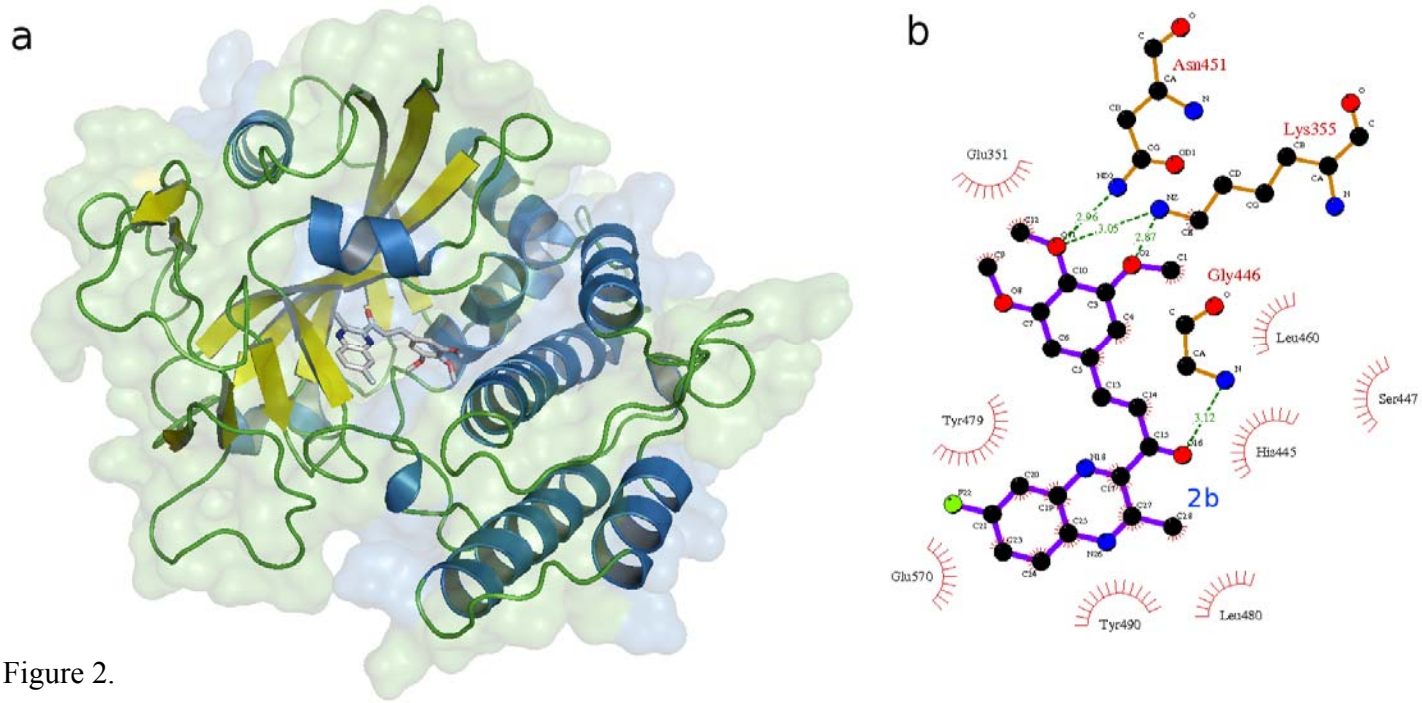

Figure 2.

(a).Molecular surface and secondary structure of catalytic domain of *T. cruzi* catPARP-1 modeled in complex with compound 2b. Alpha helix and beta sheets of the protein are in blue and yellow respectively. The backbone is green. In the centre is the quinoxaline derivative. (b) Main interactions between compound 2b (purple lines) and active site of *T.cruzi* catPARP-1 homologous protein (orange lines). Hydrophobic sandwich conformed by Tyr490 and Try479 residues, where plain lines show π-π stacking interactions. In green doted lines, hydrogen bonds and distances between oxygens of the carbonyl group (C=O- -H), methoxy (CH3-O- -H) and residues Gly446, Lys 355 and Asn451. In red lines hydrophobic residues.

Experimental section

Chemistry

The IR spectra were performed on Thermo Nicolet FT-IR Nexus Euro (Madison, USA) using KBr pellets; the frequencies are expressed in cm-1. The 1H NMR spectra were recorded on a Bruker 400 UltrashieldTM (Bruker BioSpin GmbH, Rheinstetten, Germany), using TMS as the internal standard and with CDCl3 and DMSO-d6 as the solvents; the chemical shifts are reported in ppm (d) and the coupling constant (J) values are given in Hertz (Hz). Elemental microanalyses were obtained on an Elemental Analyzer LECO CHN-900 (Michigan, USA) from vacuum-dried samples. The analytical results for C, H, and N were within ± 0.4 of the theoretical values.

Alugram® SIL G/UV254 (Layer: 0.2 mm) (Macherey-Nagel GmbH & Co. KG. Postfach 101352. D-52313 Düren, Germany) was used for Thin Layer Chromatography and Silica gel 60 (0.040-0.063 mm) for Column Flash Chromatography (Merck).

All reagents and solvents were purchased from commercial sources. E. Merck (Darmstadt, Germany), Scharlau (F.E.R.O.S.A., Barcelona, Spain), Panreac Química S.A. (Montcada Reixac, Barcelona, Spain), Sigma-Aldrich Química, S.A., (Alcobendas, Madrid), Acros Organics (Janssen Pharmaceuticalaan 3a, 2440 Geel, België) and Lancaster (Bischheim-Strasbourg, France).

Synthesis of quinoxaline and quinoxaline 1,4-di-N-oxide derivatives.

The compounds 1a-f were synthesized according to Burguete and al. (2007)[15]. The synthesis of compounds 2a-f was carried out as shown in the scheme 1. The synthesis of compounds 2a-f was carried out by previously described procedures[16].

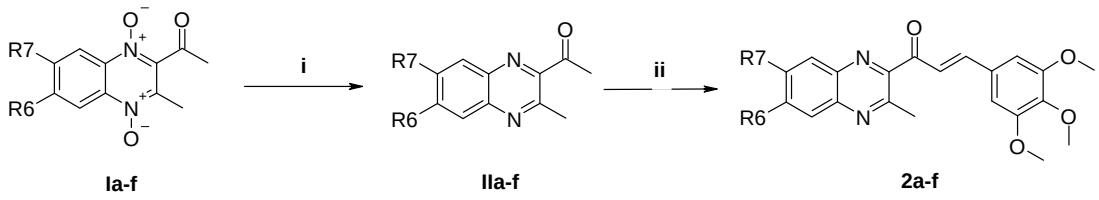

(i) $Na_2S_2O_4$, methanol, 70ºC; (ii) 3,4,5-Trimethoxy-benzaldehyde, 3% NaOH/methanol, r.t

Scheme 1. Synthesis of compounds 2a-f

Parasite and cell culture.

All chemicals were from Sigma Aldrich.

L. peruviana (MHOM/PE/LCA08) was maintained in the promastigote stage in a biphasic medium (blood agar with 0.89 % NaCl, pH 7.4) at 24 °C, with sub-passage every 3 - 4 days[17]. Axenic amastigotes transformation was then induced increasing the temperature to 34 °C and incubating during 96 h[18].

THP-1 monocytic cells (ATCC TIB-202) were maintained in 25 cm² tissue culture flasks with RPMI 1640 supplemented with 5 mM L-Glutamine, 100 U/ml penicillin, 100 µg/ml streptomycin, and 10 % foetal bovine serum (FBS) at 37 °C and 5 % CO_2

Trypanosoma cruzi (Tulahuen C4) transfected with β-galactosidase (Lac Z) gene was prepared using previously described methodology[19]. Nifurtimox was used as control.

Monolayer VERO (African Green Monkey kidney epithelial cells) and LLc-Mk2 (primary monkey kidney cells) were maintained in complete RPMI 1640 without phenol red (Sigma company, St. Louis MO), supplemented with 10% heat inactivated foetal bovine serum at 37 °C and 5% CO_2.

Murine macrophages were harvested from peritoneal cavities of 6-8 week-old female BALB/c mice in ice-cold M199 medium supplemented with 10 % FBS[20].

Screening on infected macrophages.

Extracted macrophages were immediately deposited on sterile 4 x 4 mm cover glasses and placed in each well of a 96-well plate. Plates were incubated for 24 h at 37°C, 5% CO_2 to allow cell adhesion. Pre-warmed complete M199 medium was used twice to remove non-adherent cells. Macrophages were infected according to Gonzalez et al., (2009); Ic_{50} was also calculated as the dose capable of a 50% reduction in the number of infected cells (calculated using the Excel trend formula). All experiments

were performed in triplicate. ANOVA was used to test for statistical significance of differences (Epi-Info, Statview student program). Amphotericine was used as control.

Toxicity Assay.

Differentiated murine peritoneal macrophages were treated with drugs and the trypan blue dye exclusion method was used[20]. Dilutions in complete medium were then added to achieve a final volume of 100 µl. The culture was continued for another 48 h. After this incubation, the number of viable cells was scored by hematocytometer using 0.4 % trypan blue solution in PBS. The half-maximal cytotoxic concentration 50 (Cc50) was determined.

For the cells lines (THP-1, VERO and LLc-Mk2), effect of the drugs was determinate using the 3-(4,5-dimethylthiazol-2-yl)-2,5-diphenyltetrazolium bromide (MTT) viability assay. THP-1, VERO and LLc-Mk2 cells in complete RPMI 1640 medium without phenol red were added (5x105 cells/ml, 100µl/well) to the 96-well flat-bottom plates and incubated for 48h at 37°C, 5% CO_2 with different concentrations of drugs. The MTT (25µl) was added for an additional 4h. To stop the reaction, 100µl of lyses buffer (acetic acid 1%, absolute ethanol (50/50), 20% SDS) was incubated for 15min under agitation, at room temperature. Finally, the optical density was read at 590 nm with a 96-well scanner (Bio-Rad). The experiments were repeated 3 times.

Computational Details.

Physicochemical Parameters Calculation.

Molinspiration online property calculation toolkit[21] was used to calculate Topological Polar Surface Area (TPSA)[22], the solubility expressed as the miLogP and violations of Lipinski's rule of five[23] for each of the tested compound. Absorption (%ABS) was calculated by: $\%ABS = 109 - (0.345 \times TPSA)$[24].

Screening of proteins co-crystallized with quinoxaline family compounds and T.cruzi crystallized proteins.

The Protein Data Bank database was screened for the presence of crystallized proteins in complex with quinoxaline-type compounds. The search was performed manually using "quinoxaline" as advance mode keyword. In the same way, a search of *T.cruzi* crystallized proteins was performed (reported until 05/2009).

***T. cruzi* homologue proteins.**

T. cruzi homologues of the PDB-proteins crystallized in complex with quinoxaline-type compounds were identified in the Sanger Institute *T. cruzi* genome database and in the Genebank using Blastp. An E-value less than 1e-10 was used as the critical point to establish homology. In case a homologue was not found, we looked for other available *T. cruzi* proteins that belonged to the same protein family.

Homology modeling of *T. cruzi* PARP-1.

An homology structure model of the catalytic domain of *T. cruzi* PARP-1 was obtained by submitting a manually edited pair wise sequence alignment of the human PARP-1 to the Swiss-model server[25-27]. The sequence alignment was made with T-coffee[26] server following the structure information reported in previous works[11-13]. The 44% identical human PARP-1 crystal structure (PDB ID: 1wok, 3 Å resolution) was used as template. To refine the structure model, energy minimization using the steepest descent method was performed, followed by 50 ps of stabilization at constant temperature (310 K), and 1 ns of molecular dynamics (MD) using the software GROMACS[28]. The accuracy of the model was evaluated with the PROCHECK[29] and WHAT-CHECK[30] servers.

Ligand preparation.

The three-dimensional structures and atomic coordinates of the second series of quinoxalines (2a-f) were obtained using the molecular modeling software, Hyperchem 7.5[31] (see supporting information).

Analysis Detection of potential candidate targets for 2a-f Quinoxalines.

The molecular docking program Autodock 4.0 [32] was used to determine the most likely configuration of the binding of each compound with the selected quinoxaline candidate targets.The best binding configuration was selected by choosing the conformation with conserved interactions as previously described[7, 11-13] and the minimum Gibbs free energy associated. Further details on computational protocols are in supporting information.

Acknowledgments

The authors thank Professor Jorge Arévalo of the Instituto de Medicina Tropical ‘‘Alexander von Humboldt” of the Universidad Peruana Cayetano Heredia, for providing THP-1 cells and *L. peruviana* LCA 08 strain.

Supporting Information Available : Computational details and Autodock calculations of the *T.cruzi* proteins.This material is available free of charge via the Internet at http://pubs.acs.org

Supporting Information.

Computational Details.

Ligand structures were sketched using Hyperchem 7.5 and minimized with an implemented version of MM+ force field kindly using the steepest descent and Polak-Ribiere conjugated gradient method (0.001 kJ/mol·Å convergence). MM+ is an all-atom force field based on the MM2 functional form. The resulting minimized conformation was then submitted to molecular docking simulations. To be exported to Autodock, the minimized structures were converted into the pdb file format using Hyperchem software.

Autodock calculations.

To prepare the input structures for Autodock calculations, the structures of catPARP-1, arginine kinase and glucokinase of *T. cruzi* were further manipulated by adding Kollman partial charges and

solvent parameters. Similarly to the protein, the structure of the inhibitors was also prepared by deleting their nonpolar hydrogen atoms and adding Gasteiger atomic charges. Finally, the rigid root and rotatable bonds were defined using AutoDockTools.

Autogrid 4.0, as implemented in the Autodock 4.0 software package, was used to generate grid maps. The Lamarckian genetic algorithm (LGA) was employed to generate orientations/conformations of the ligand within the binding site. The crystallographic complex between 1WOK and CNQ was used to check the ability of the program Autodock to investigate the binding mode of inhibitors into the binding site of the enzyme. For this purpose, the complex was manipulated to extract the inhibitor, which was in turn computationally re-docked by means of Autodock within the binding site. A grid point spacing of 0.375 Å and 80 × 80 × 80 points were used. The grid was centered on the mass center of the crystallographic inhibitor. The program successfully reproduced the X-ray coordinates of the inhibitor's binding conformation with a rmsd (0.8 Å). Different Autodock parameter files were set to choose the optimal conformation.

outlev 1	diagnostic output level
rmstol 2.0	cluster_tolerance/A
extnrg 1000.0	external grid energy
e0max 0.0 10000	max initial energy; max number of retries
ga_pop_size 150	number of individuals in population
ga_num_evals 250000	maximum number of energy evaluations
ga_num_generations 27000	maximum number of generations
ga_elitism 1	number of top individuals to survive to next generation
ga_mutation_rate 0.02	rate of gene mutation

ga_crossover_rate 0.8	rate of crossover
ga_cauchy_alpha 0.0	Alpha parameter of Cauchy distribution
ga_cauchy_beta 1.0	Beta parameter Cauchy distribution
set_ga	set the above parameters for GA or LGA
sw_max_its 300	iterations of Solis & Wets local search
sw_max_succ 4	consecutive successes before changing rho
sw_max_fail 4	consecutive failures before changing rho
sw_rho 1.0	size of local search space to sample
sw_lb_rho 0.01	lower bound on rho
ls_search_freq 0.06	probability of performing local search on individual
set_psw1	set the above pseudo-Solis & Wets parameters
ga_run 100	do this many hybrid GA-LS runs
analysis	perform a ranked cluster analysis

References:

1. Davis, A. J.; Murray, H. W.; Handman, E. Drugs against leishmaniasis: a synergy of technology and partnerships. *Trends Parasitol* **2004,** 20, 73-6.
2. Soto, J.; Rea, J.; Balderrama, M.; Toledo, J.; Soto, P.; Valda, L.; Berman, J. D. Efficacy of miltefosine for Bolivian cutaneous leishmaniasis. *Am J Trop Med Hyg* **2008,** 78, 210-1.
3. Yardley, V.; Croft, S. L.; de Doncker, S.; Dujardin, J. C.; Koirala S; Rijal, S.; Miranda, C.; Llanos-Cuentas, A.; Chappuis, F. The sensitivity of clinical isolates of Leishmania from Peru and Nepal to miltefosine. *Am J Trop Med Hyg* **2005,** 73, 272-275.
4. Nwaka, S.; Hudson, A. Innovative lead discovery strategies for tropical diseases. *Nat Rev Drug Discov* **2006,** 5, 941-55.
5. Burguete, A.; Estevez, Y.; Castillo, D.; Gonzalez, G.; Villar, R.; Solano, B.; Vicente, E.; Silanes, S. P.; Aldana, I.; Monge, A.; Sauvain, M.; Deharo, E. Anti-leishmanial and structure-activity relationship of ring substituted 3-phenyl-1-(1,4-di-N-oxide quinoxalin-2-yl)-2-propen-1-one derivatives. *Mem Inst Oswaldo Cruz* **2008,** 103, 778-80.
6. Ishida, J.; Yamamoto, H.; Kido, Y.; Kamijo, K.; Murano, K.; Miyake, H.; Ohkubo, M.; Kinoshita, T.; Warizaya, M.; Iwashita, A.; Mihara, K.; Matsuoka, N.; Hattori, K. Discovery of potent

and selective PARP-1 and PARP-2 inhibitors : SBDD analysis via a combination of X-ray structural study and homology modeling. *Bioorg. Med. Chem.* **2006,** 14, 1378–1390.
7. Iwashita, A.; Hattori, K.; Yamamoto, H.; Ishida, J.; Kido, Y.; Kamijo, K.; Murano, K.; Miyake, H.; Kinoshita, T.; Warizaya, M.; Ohkubo, M.; Matsuoka, N.; Mutoh, S. Discovery of quinazolinone and quinoxaline derivatives as potent and selective poly(ADP-ribose) polymerase-1/2 inhibitors. *FEBS Letters* **2005**, 1389-1393.
8. Fernandez Villamil, S. H.; Baltanas, R.; Alonso, G. D.; Vilchez Larrea, S. C.; Torres, H. N.; Flawia, M. M. TcPARP : A DNA damage-dependent poly(ADP-ribose)polymerase from *Trypanosoma cruzi*. *International Journal for Parasitology* **2008,** 38, 277-287.
9. Caceres, A. J.; Quinones, W.; Gualdron, M.; Cordeiro, A.; Avilan, L.; Michels, P. A.; Concepcion, J. L. Molecular and biochemical characterization of novel glucokinases from Trypanosoma cruzi and Leishmania spp. *Mol Biochem Parasitol* **2007,** 156, 235-45.
10. Pereira, C. A.; Alonso, G. D.; Paveto, M. C.; Iribarren, A.; Cabanas, M. L.; Torres, H. N.; Flawia, M. M. Trypanosoma cruzi arginine kinase characterization and cloning. A novel energetic pathway in protozoan parasites. *J Biol Chem* **2000,** 275, 1495-501.
11. Kinoshita, T.; Nakanishi, I.; Warizaya, M.; Iwashita, A.; Kido, Y.; Hattori, K.; Fujii, T. Inhibitor-induced structural change of the active site of human poly(ADP-ribose) polymerase. *FEBS Lett* **2004,** 556, 43-6.
12. Costantino, G.; Macchiarulo, A.; Camaioni, E.; Pellicciari, R. Modeling of poly(ADP-ribose)polymerase (PARP) inhibitors. Docking of ligands and quantitative structure-activity relationship analysis. *J Med Chem* **2001,** 44, 3786-94.
13. Ruf, A.; Mennissier de Murcia, J.; de Murcia, G.; Schulz, G. E. Structure of the catalytic fragment of poly(AD-ribose) polymerase from chicken. *Proc Natl Acad Sci U S A* **1996,** 93, 7481-5.
14. Dundas, J.; Ouyang, Z.; Tseng, J.; Binkowski, A.; Turpaz, Y.; Liang, J. CASTp: computed atlas of surface topography of proteins with structural and topographical mapping of functionally annotated residues. *Nucleic Acids Res* **2006,** 34, W116-8.
15. Burguete, A.; Pontiki, E.; Hadjipavlou-Litina, D.; Villar, R.; Vicente, E.; Solano, B.; Ancizu, S.; Perez-Silanes, S.; Aldana, I.; Monge, A. Synthesis and anti-inflammatory/antioxidant activities of some new ring substituted 3-phenyl-1-(1,4-di-N-oxide quinoxalin-2-yl)-2-propen-1-one derivatives and of their 4,5-dihydro-(1H)-pyrazole analogues. *Bioorg Med Chem Lett* **2007,** 17, 6439-43.
16. Burguete, A. Design, synthesis and biological evalulation of new quinoxaline and quinoxaline 1,4-di-N-oxide derivatives with application in different therapeutic areas. Universidad de Navarra Spain, Pamplona, 2010.
17. Gonzalez, G.; Castillo, D.; Estevez, Y.; Grentzinger, T.; Deharo, E. Leishmania (Viannia) peruviana (MHOM/PE/LCA08): comparison of THP-1 cell and murine macrophage susceptibility to axenic amastigotes for the screening of leishmanicidal compounds. *Exp Parasitol* **2009,** 122, 353-6.
18. Teixeira, M.; de Jesus Santos, R.; Sampaio, R.; Pontes-de-Carvalho, L.; dos-Santos, W. A simple and reproducible method to obtain large numbers of axenic amastigotes of different Leishmania species. *Parasitology Research* **2002,** 88, 963-968.
19. Aponte, J. C.; Verastegui, M.; Malaga, E.; Zimic, M.; Quiliano, M.; Vaisberg, A. J.; Gilman, R. H.; Hammond, G. B. Synthesis, cytotoxicity, and anti-Trypanosoma cruzi activity of new chalcones. *J Med Chem* **2008,** 51, 6230-4.
20. Castillo, D.; Arevalo, J.; Herrera, F.; Ruiz, C.; Rojas, R.; Rengifo, E.; Vaisberg, A.; Lock, O.; Lemesre, J. L.; Gornitzka, H.; Sauvain, M. Spirolactone iridoids might be responsible for the antileishmanial activity of a Peruvian traditional remedy made with Himatanthus sucuuba (Apocynaceae). *J Ethnopharmacol* **2007,** 112, 410-4.
21. MolinspirationCheminformatics, Bratislava, SlovakRepublic. http://www.molinspiration.com/services/properties.html (January 16, 2009).
22. Ertl, P.; Rohde, B.; Selzer, P. Fast calculation of molecular polar surface area as a sum of fragment-based contributions and its application to the prediction of drug transport properties. *J Med Chem* **2000,** 43, 3714-7.

23. Lipinski, C. A.; Lombardo, F.; Dominy, B. W.; Feeney, P. J. Experimental and computational approaches to estimate solubility and permeability in drug discovery and development settings. *Adv Drug Deliv Rev* **2001,** 46, 3-26.
24. Zhao, Y. H.; Abraham, M. H.; Le, J.; Hersey, A.; Luscombe, C. N.; Beck, G.; Sherborne, B.; Cooper, I. Rate-limited steps of human oral absorption and QSAR studies. *Pharm Res* **2002,** 19, 1446-57.
25. Arnold, K.; Bordoli, L.; Kopp, J.; Schwede, T. The SWISS-MODEL workspace: a web-based environment for protein structure homology modelling. *Bioinformatics* **2006,** 22, 195-201.
26. Guex, N.; Peitsch, M. C. SWISS-MODEL and the Swiss-PdbViewer: an environment for comparative protein modeling. *Electrophoresis* **1997,** 18, 2714-23.
27. Schwede, T.; Kopp, J.; Guex, N.; Peitsch, M. C. SWISS-MODEL: An automated protein homology-modeling server. *Nucleic Acids Res* **2003,** 31, 3381-5.
28. Hess, B.; Kutzner, C.; van der Spoel, D.; Lindahl, E. GROMACS 4: Algorithms for Highly Efficient, Load-Balanced, and Scalable Molecular Simulation. *Journal of Chemical Theory and Computation* **2008,** 4, 435-447.
29. PROCHECK: a program to check the stereochemical quality of protein structures. *Journal of Applied Crystallography* **1993,** 26, 283-291.
30. Hooft, R. W.; Vriend, G.; Sander, C.; Abola, E. E. Errors in protein structures. *Nature* **1996,** 381, 272.
31. Hypercube. *HyperChem 7.5*, Ontario.
32. Morris, G. M.; Huey, R.; Lindstrom, W.; Sanner, M. F.; Belew, R. K.; Goodsell, D. S.; Olson, A. J. AutoDock4 and AutoDockTools4: Automated docking with selective receptor flexibility. *J Comput Chem* **2009**.
33. Gordon, L. F. Substituent constants for correlation analysis in chemistry and biology. By Corwin Hansch and Albert Leo. Wiley, 605 Third Ave., New York, NY 10016. 1979. 339 pp. 21 × 28 cm. Price $24.95. *Journal of Pharmaceutical Sciences* **1980,** 69, 1109.

Table 1. Biological activities of quinoxaline derivatives

			Cc50 (µM)[a]				Ic50 (µM)[b]	
Compounds	**R7**	**R6**	**M.P.M[c]**	**Thp-1[d]**	**VERO[e]**	**LLc-Mk2[f]**	***L. peruviana***	***T. cruzi***
1a	-	-	116.2	98.1	93.8	134.0	27.5	>25
1b	F	-	130.2	40.0	112.0	78.2	13.7	>25
1d	CH3	-	113.9	53.2	>235.6	>235.6	8.9	>25
1e	O-CH3	-	136.6	107.8	>227.0	>227.0	28.5	>25
1f	CH3	CH3	63.2	28.9	61.6	75.3	ND[g]	22.8
2a	-	-	9.3	2.7	7.9	11.9	9.4	18.3
2b	F	-	279.5	15.2	21.3	16.3	2.8	14.3
2c	Cl	-	332.5	19.7	117.7	99.4	21.4	>25
2d	CH3	-	61.8	4.4	16.5	22.0	11.9	16.5
2e	O-CH3	-	11.3	1.4	7.6	10.1	1.2	11.5
2f	CH3	CH3	287.9	38.0	>254.8	>254.8	12.7	>25
Amp B[h]			5.5	>50	24.4	ND	0.10	-
Nifurtimox							-	4.5

[a]Ic_{50}: concentration that produces 50% inhibitory effect. [b]Cc_{50}: concentration that produces 50% cytotoxic effect. [c]Murine Peritoneal Macrophages. [d]human monocytic cells. [e,f]monkey kidney cells.[g]ND: Not Determined. [h]Amphotericin B was used as control.Values represent the average of three determinations (one determination of three independent experiments).Errors for individual measurements differed by less than 50%.

Table 2. Physical Chemical Properties of derivatives Quinoxalines[a]

ID rule	%ABS	TPSA (Å) ≤140	*n*-RT	Molecular weight <500	miLog*P* <5	Lipophilicity ($\Sigma\pi$)[b]	N H-bond donors ≤5	N H-bond acceptors ≤10	Lipinski's violations ≤1
1a	73.47	103	5	410.43	-0.06	0	1	9	0
1b	73.47	103	5	428.42	0.08	0.14	1	9	0
1d	73.47	103	5	424.46	0.37	0.42	1	9	0
1e	70.29	112.2	6	440.46	-0.03	0.03	1	10	0
1f	73.47	103	5	438.49	0.74	0.8	1	9	0
2a	84.68	70.5	6	364.4	3.70	0	0	6	0
2b	84.68	70.5	6	382.39	3.84	0.14	0	6	0
2c	84.68	70.5	6	398.85	4.35	0.65	0	6	0
2d	84.68	70.5	6	378.43	4.12	0.42	0	6	0
2e	81.50	79.7	7	394.43	3.73	0.03	0	7	0
2f	84.68	70.5	6	392.46	4.50	0.8	0	6	0

[a] %ABS, percentage of absorption, calculated by: %ABS = 109 – (0.345 x TPSA); TPSA, topological polar surface area; n-RT, number of rotable bonds; miLogP, logarithm of compounds partition coefficient between n-octanol and water. [b] Relative lipophilicities determined by computation of π values for all 1 or 2 and nuclear substituents using the fragment constant method[33]. These calculations are for the free base forms of potentially cationic side chains.

Table 3. Autodock binding energies between quinoxalines derivates serie 2 and potential targets in *T.cruzi*.

Enzyme	Total Autodock energy (Kcal/mol) for compounds 2a-2f					
	2a	**2b**	**2c**	**2d**	**2e**	**2f**
catPARP-1	-4.8	-4.78	-5.48	-5.27[a]	-4.95[a]	-5.6
Arginine Kinase	-3.99	-3.96	-4.34	-4.28	-4.02	-3.77
Glucokinase	-4.05	-4.03	-3.84	-3.81	-3.60[a]	-4.44[a]

[a] No conserved interactions with inhibitors or substrates. Only energies associated with best docking conformation.